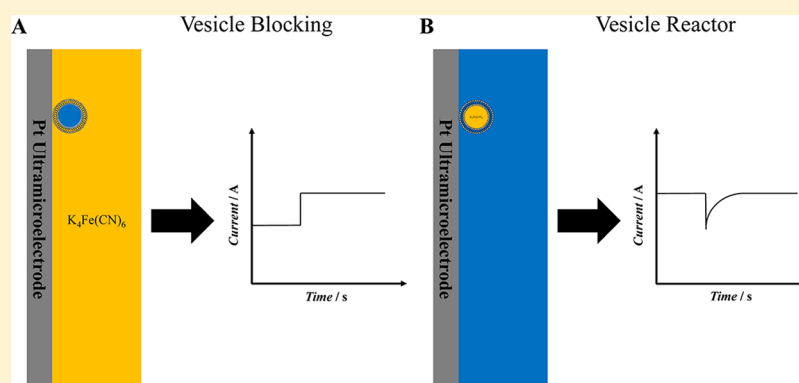


# Electrochemical Detection of Single Phospholipid Vesicle Collisions at a Pt Ultramicroelectrode

Estelle Lebègue,<sup>†,‡</sup> Cari M. Anderson,<sup>‡</sup> Jeffrey E. Dick,<sup>†,‡</sup> Lauren J. Webb,<sup>‡</sup> and Allen J. Bard<sup>\*,†,‡</sup>

<sup>†</sup>Center for Electrochemistry and <sup>‡</sup>Department of Chemistry, The University of Texas at Austin, Austin, Texas 78712, United States

## S Supporting Information



**ABSTRACT:** We report the collision behavior of single unilamellar vesicles, composed of a bilayer lipid membrane (BLM), on a platinum (Pt) ultramicroelectrode (UME) by two electrochemical detection methods. In the first method, the blocking of a solution redox reaction, induced by the single vesicle adsorption on the Pt UME, can be observed in the amperometric  $i-t$  response as current steps during the electrochemical oxidation of ferrocyanide. In the second technique, the ferrocyanide redox probe is directly encapsulated inside vesicles and can be oxidized during the vesicle collision on the UME if the potential is poised positive enough for ferrocyanide oxidation to occur. In the amperometric  $i-t$  response for the latter experiment, a current spike is observed. Here, we report the vesicle blocking (VB) method as a relevant technique for determining the vesicle solution concentration from the collisional frequency and also for observing the vesicle adhesion on the Pt surface. In addition, vesicle reactor (VR) experiments show clear evidence that the lipid bilayer membrane does not collapse or break open at the Pt UME during the vesicle collision. Because the bilayer is too thick for electron tunneling to occur readily, an appropriate concentration of a surfactant, such as Triton X-100 (TX100), was added in the VR solution to induce loosening of the bilayer (transfection conditions), allowing the electrode to oxidize the contents of the vesicle. With this technique, the TX100 effect on the vesicle lipid bilayer permeability can be evaluated through the current spike charge and frequency corresponding to redox vesicle collisions.

## INTRODUCTION

Electrochemical detection of discrete soft nanoparticle collisions on ultramicroelectrodes (UMEs) has been recently reported as a method to determine the size distribution and the concentration of emulsion droplets,<sup>1–5</sup> vesicles,<sup>6,7</sup> viruses,<sup>8</sup> micelles,<sup>9</sup> and biological macromolecules.<sup>10</sup> The observation of these stochastic events can potentially provide information on various single nanoparticles contrary to ensemble measurements.<sup>11</sup> Especially, electrochemical detection by collisions has been extended to studying vesicles by oxidizing the contents released upon collision at a carbon UME.<sup>6,7</sup> There is, however, lack of agreement about the membrane opening mechanism followed by the content electrolysis on the carbon UME. Compton and co-workers proposed a “full collapse fusion” mechanism of the liposome membrane during the collision, based on the complete release and oxidation of ascorbic acid in a commercial vitamin C preparation, on a carbon UME.<sup>6</sup> In contrast, Ewing and co-workers proposed a mechanism where

the vesicle first adsorbs to the electrode surface and spreads out over the electrode, and finally the oxidation of the catecholamine content occurs.<sup>7</sup> Moreover, this process is supported by previous investigations from Kasemo and co-workers about vesicles adsorption on various substrates (silicon dioxide, thiolated gold, oxidized gold) where the authors reported a rupture of vesicles adsorbed on hydrophobic surfaces (thiolated gold) and, by opposition, an adsorption of intact vesicles on more hydrophilic surfaces (oxidized gold).<sup>12,13</sup> In the same trend, Scholz and co-workers studied the behavior of different liposomes on the electrode surface (mainly a mercury electrode) and showed that chronoamperometric measurements are an interesting tool to probe the membrane stability and to understand the effect of its properties on vesicle

Received: August 21, 2015

Revised: October 7, 2015

Published: October 8, 2015

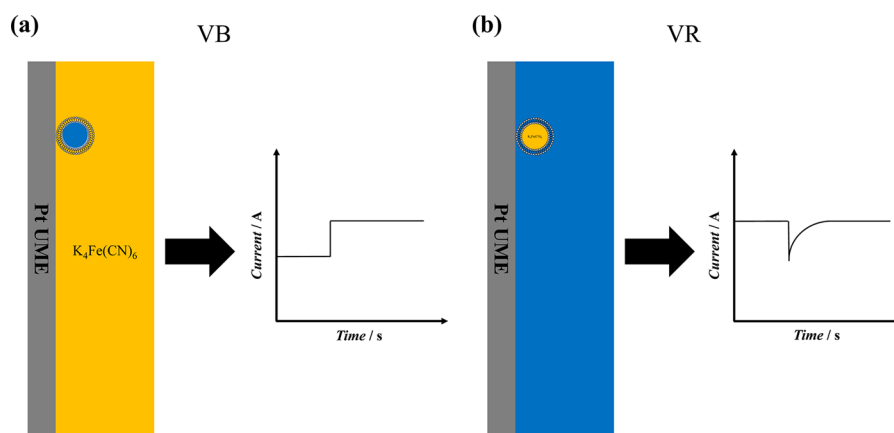


**Figure 1.** Schematic representation of the two reported vesicle collision techniques at a Pt UME where the potential applied is at +0.6 V vs Ag/AgCl, and the oxidation currents are plotted in the negative direction (a) Electrochemical oxidation of  $\text{Fe}(\text{CN})_6^{4-}$  in aqueous solution (negative current) is partially blocked by single vesicle blocking (VB) which produces an anodic current step. (b) Electrochemical oxidation of  $\text{Fe}(\text{CN})_6^{4-}$  encapsulated inside the vesicle reactor (VR) gives an anodic current spike.

fusion.<sup>14–17</sup> In particular, the authors were the first to study the adhesion and bursting processes of 450 nm diameter liposomes and the spreading of the lecithin on the mercury surface (0.48 mm<sup>2</sup>) by using chronoamperometric measurements for determining the frequency of spikes and the charge densities of formed monolayers.<sup>14–16</sup>

To improve our understanding of vesicle interactions with an electrode surface, we herein present different vesicle behavior on a Pt UME, which serves as a hydrophilic surface for vesicle collisions. By analogy with emulsion results,<sup>1–4</sup> we report two techniques of vesicle detection: (1) vesicle blocking (VB), which consists of observing a blocking of solution redox species due to the single vesicle adsorption on the UME, and (2) vesicle reactor (VR), where the redox probe is encapsulated inside the vesicle and can be electrolyzed at the UME after its collision (Figure 1). In both cases, the redox probe chosen was potassium ferrocyanide [ $\text{K}_4\text{Fe}(\text{CN})_6$ ]<sup>18</sup> because of its high solubility in water (0.5 M). Moreover, 0.5 M  $\text{K}_4\text{Fe}(\text{CN})_6$  can be easily encapsulated inside vesicles as a hydrophilic content and removed from the solution outside vesicles. Also, it is a relevant redox species for the continuous phase largely used for detection of various soft nanoparticle collisions by the blocking method.<sup>1,8,10</sup>

Here we demonstrate that the BLM does not break and release the contents during vesicle collision at the Pt UME hydrophilic surface. As shown in previous studies of BLMs,<sup>19,20</sup> they do not allow effective electron tunneling or ion transport to cause redox reactions across them without the presence of a strong surfactant. However, cell transfection experiments show that the presence of a surfactant, e.g., Triton X-100 (TX100), can promote transfer across the membrane.<sup>18,21</sup> Moreover, we clearly show that vesicles are adsorbed on the Pt surface (VB) after their collision, but the electron transfer cannot happen through the bilayer for electrolyzing the  $\text{Fe}(\text{CN})_6^{4-}$  content (VR). Hence, we discuss here the TX100 concentration effect in solution and also the corresponding kinetic study on the vesicle membrane permeability by detection of electrochemical collision events. Our results were in good agreement with several studies reporting the role of TX100 surfactant on the cell membrane, which could yield fundamental insight into the transfection process.<sup>21–25</sup> To the best of our knowledge, this is the first work dealing with the vesicle collision behavior onto a hydrophilic surface.

## EXPERIMENTAL SECTION

**Reagents.** All chemicals were reagent grade and used as purchased without further purification. Water used in each experiment was Milli-Q water. Chloroform ( $\geq 99.8\%$ ), sulfuric acid (97%), and hydrogen peroxide (30%) were obtained from Fisher Scientific. Ferrocenemethanol (97%), potassium ferrocyanide, potassium phosphate monobasic ( $\geq 99.0\%$ ), potassium phosphate dibasic ( $\geq 98\%$ ), and Triton X-100 were purchased from Sigma-Aldrich. Pt (99.9%) wire was obtained from Goodfellow (Devon, PA). 1,2-Dimyristoyl-*sn*-glycero-3-phosphocholine (DMPC) lipids were purchased in powder from Avanti Polar Lipids and stored in a freezer.

**Vesicle Preparation.** Unilamellar vesicle solutions were prepared by dissolution of 10 mM DMPC lipid (powder) in chloroform (1 mL), then vortexed for 5 min, and placed into a warm water bath (40 °C) for at least 10 min until the complete dissolution of lipids. The homogeneous mixture was placed under ambient atmosphere overnight and then under vacuum for 1 h for the complete evaporation of chloroform. The dry lipid film was hydrated by addition of aqueous solution (2 mL of pure water or 2 mL of 0.5 M  $\text{K}_4\text{Fe}(\text{CN})_6$  aqueous solution), and then the solution was mixed for 5 min and heated on a hot plate at 40 °C for 30 min. The DMPC vesicle solutions were extruded using 400, 200, and finally 100 nm diameter polycarbonate membranes. The vesicle solution was passed through the extruder, which was kept warm at 40 °C 10 times (for each polycarbonate membrane size) to obtain monodisperse nanometer-sized DMPC unilamellar vesicles. The final step was to pass the DMPC vesicle solution through a column (PD-10 Desalting Columns, GE Healthcare) by using pure water for removing  $\text{K}_4\text{Fe}(\text{CN})_6$  outside vesicles.

**Materials and Instrumentation.** The vesicles extrusion phase was carried out with the extruder set from Avanti Polar Lipids including a mini-extruder, two syringes of 1 mL, polycarbonates membranes of 0.4, 0.2, and 0.1  $\mu\text{m}$ , and filter supports. The electrochemical experiments were performed using a CHI model 920C and CHI630 potentiostat (CH Instruments, Austin, TX) with a three-electrode cell placed in a faraday cage. Platinum wire was used as a counter electrode, and the reference electrode was Ag/AgCl. For all chronoamperometric *i*-*t* curves recorded, the sample interval (in sampling time) was 50 ms. Dynamic light scattering (DLS) data were obtained by Zetasizer Nano ZS (Malvern, Westborough, MA), and nanoparticle tracking analysis (NTA) data was achieved by Nanosight. However, this last one (NTA) was discontinued when we found fouling of the cell window. The size distribution of vesicles was analyzed by DLS in Figure S1 and NTA in Figure S2, both in agreement with  $120 \pm 30$  nm diameter DMPC vesicles aqueous solutions.

Platinum ultramicroelectrodes were prepared by laser pulling (Sutter Instruments) according to the general procedure performed

in our lab,<sup>26,27</sup> followed by mechanical polishing with Bevelers for a diameter between 1 and 2  $\mu\text{m}$ . Before each experiment, the Pt UMEs were washed by dipping in piranha solution (mixture composed to 3:1 concentrated sulfuric acid to 30% hydrogen peroxide solution) for 10 s, then dipping in water, and finally dipping successively in acetone, ethanol, and several times in water. The radius of the Pt UME was obtained using the steady-state current in cyclic voltammetry recorded in 1 mM ferrocenemethanol aqueous solution.

## RESULTS AND DISCUSSION

**VB Method.** The electrochemical detection of collisions by the VB method is presented in Figure 2. The potential applied

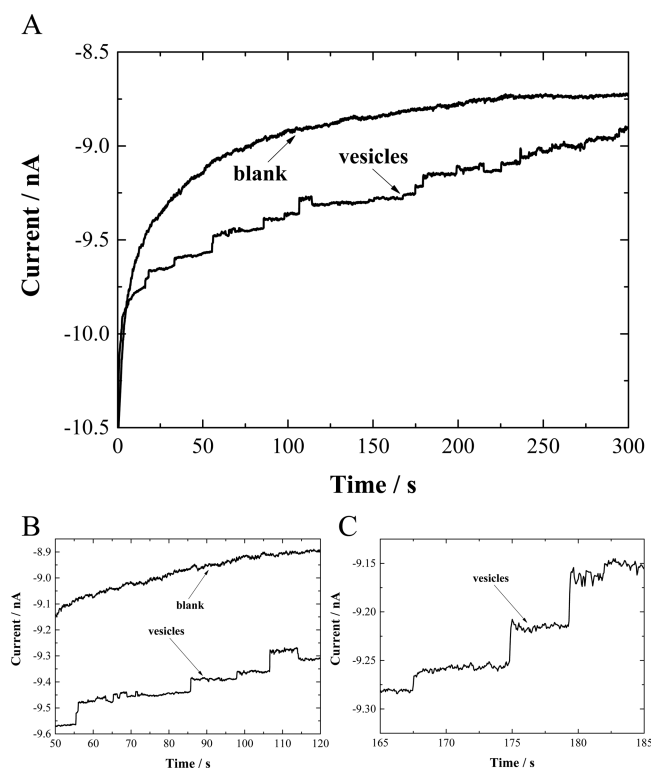


**Figure 2.** (A) The  $i-t$  curve for collision experiments by vesicles blocking method recorded at +0.6 V vs Ag/AgCl on 1.7  $\mu\text{m}$  Pt UME in 2 mL of 0.2 M  $\text{K}_4\text{Fe}(\text{CN})_6$  aqueous solution in the absence (blank) and in the presence (vesicles) of 5  $\mu\text{L}$  of DMPC vesicles aqueous solution. (B) and (C) are enlarged portions of the initial figure (A).

at 0.6 V corresponding to the steady-state current of the  $\text{Fe}(\text{CN})_6^{4-}$  oxidation into  $\text{Fe}(\text{CN})_6^{3-}$  at a 1.7  $\mu\text{m}$  Pt UME was previously determined by cyclic voltammetry (Figure S3). During the chronoamperometry measurement at 0.6 V in 0.2 M  $\text{K}_4\text{Fe}(\text{CN})_6$  in the absence of DMPC vesicles, a steady-state current was reached at the Pt UME, and no current step was observed over 300 s. In contrast, after addition of DMPC vesicles encapsulating only pure water (no electroactive species), several current steps were observed due to single vesicle collisions onto the Pt UME surface, which locally block the flux of  $\text{Fe}(\text{CN})_6^{4-}$  to the electrode surface.

The experimentally observed frequency of current steps at the Pt UME with the VB method was 0.12 Hz. The vesicles concentration ( $C_{\text{ves}}$ ) can be calculated from this collision frequency of vesicles onto the UME surface by eq 1, based on a diffusion-limited flux of nanoparticles to the electrode surface.<sup>28</sup> The concentration of the pure DMPC vesicles aqueous solution before dilution is evaluated as  $5.5 \pm 0.2$  nM, a value in good

agreement with the concentration determined by NTA (Figure S2) at  $3.1 \pm 0.2$  nM, suggesting that diffusion is the dominant process compared with migration effects.<sup>29</sup> A small contribution of mass transfer of the vesicles to the electrode surface by electrophoretic migration cannot be ruled out; however, because the concentration of potassium ferrocyanide is 0.2 M, it likely carries most of the current, making diffusion the predominate form of mass transfer.<sup>8</sup>

$$C_{\text{ves}} = \frac{f_{\text{ves}}}{4D_{\text{ves}}r_eN_A} \quad (1)$$

where  $f_{\text{ves}}$  is the collision frequency by diffusion of the vesicles to the UME,  $D_{\text{ves}}$  is the diffusion coefficient of a spherical vesicle,  $r_e$  is the radius of the working electrode, and  $N_A$  is Avogadro's number. The diffusion coefficient ( $D_{\text{ves}}$ ) can be estimated by the Stokes–Einstein relation (eq 2)<sup>30</sup>

$$D_{\text{ves}} = \frac{k_B T}{6\pi\eta r_{\text{ves}}} \quad (2)$$

where  $k_B$  is Boltzmann's constant,  $T$  is temperature,  $\eta$  is the viscosity of the continuous phase at 25  $^\circ\text{C}$ , and  $r_{\text{ves}}$  is the hydrodynamic radius of a vesicle. From this equation, the diffusion coefficient of a 113 nm diameter vesicle (determined by DLS measurement in Figure S1) is  $4.3 \times 10^{-8}$   $\text{cm}^2 \text{s}^{-1}$ , matching well with the value estimated from NTA data (Figure S2) at  $4.1 \times 10^{-8}$   $\text{cm}^2 \text{s}^{-1}$ .

The current steps shown in Figure 2 are related to the single vesicle collisions at the Pt UME surface. In most cases, we observed a current decrease in the shape of a stair step, indicating that most of the vesicles stick on the Pt surface after collision and only in rare cases they quickly leave the UME after collision, showing a current increase in the shape of a stair step. Because of these observations, we assume that the probability of the adsorbate sticking to the electrode is nearly 1. Therefore, the VB electrochemical method is a relevant technique to detect nanometer-sized vesicles at a Pt UME and can give some interesting information such as the vesicles solution concentration and also information on the vesicle's adhesion on the Pt surface. The sharpness of the steps (rise time 0.25 s) suggests that any vesicle distortion or spreading either occurs very quickly or, more likely, that the vesicle maintains its essentially spherical shape.

**VR Method.** The electrochemical detection of collisions by vesicle reactor method is presented in Figure 3. The main observation in Figure 3 was the absence of current spikes in the chronoamperometric  $i-t$  curve recorded in the presence of DMPC vesicles without surfactant. Indeed, this curve showed a similar shape to the one recorded in potassium phosphate buffer (KPB) aqueous solution (in the absence of vesicles solution) with the same trend to reach the steady-state current. This result shows no oxidation of the vesicles content occurred during each collision, suggesting no lipid bilayer collapse against the Pt UME. According to the VB method applied to redox DMPC vesicles (Figure S4), we can affirm that vesicles irreversibly adsorb onto the Pt UME, but the VR technique presented in Figure 3 clearly demonstrated that electron transfer does not occur through the BLM because electron tunneling and ion transfer are not facile through such a thick barrier.<sup>19,20,31</sup> Thus, in agreement with previous studies about the vesicle adsorption on various substrates,<sup>12,13</sup> DMPC vesicles seem to remain intact during their collision on the Pt UME hydrophilic surface.

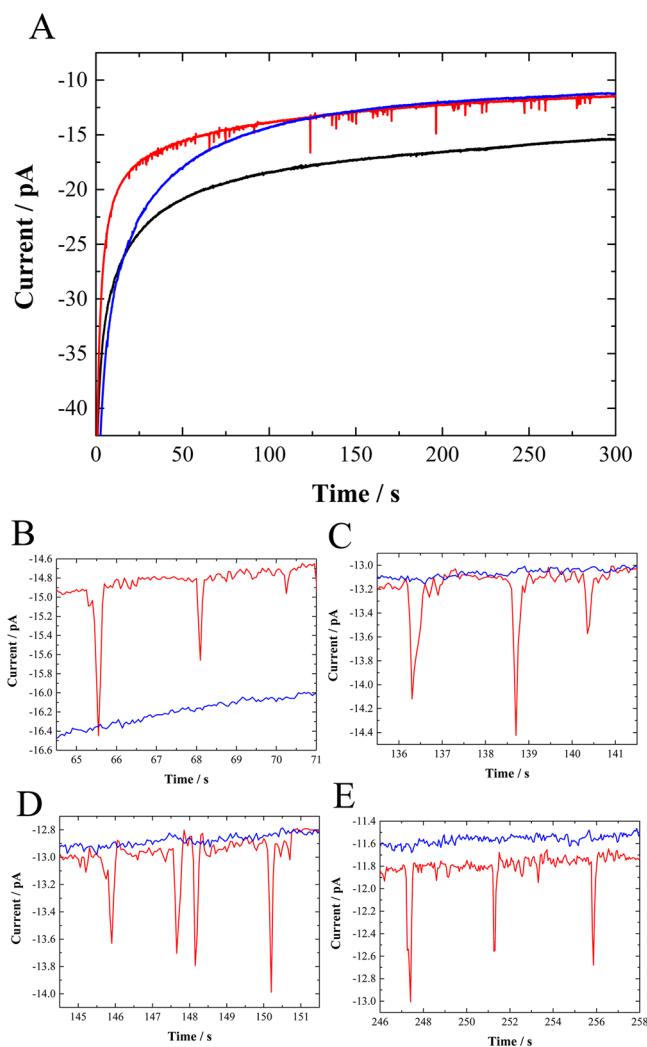


**Figure 3.** The  $i-t$  curve for collision experiments by vesicles reactor method recorded at +0.6 V vs Ag/AgCl on 1.7  $\mu\text{m}$  Pt UME in 2 mL of 0.1 M KPB aqueous solution at pH 7 in the absence (black) and in the presence of 20  $\mu\text{L}$  of redox DMPC vesicles aqueous solution with (red) and without (blue) addition of 0.2 mM Triton X-100 surfactant. (B–E) are enlarged portions of the initial figure (A).

In this case, to increase the membrane permeability, the use of a surfactant was required. The  $i-t$  curve recorded immediately after addition of an appropriate concentration of TX100 (*vide infra*, Figure 4) showed several current spikes over 300 s (Figure 3) with a frequency estimated at 0.28 Hz. Note the narrow shape of these current spikes detected at Pt UME, which are clearly different than those observed in previous studies.<sup>6,7</sup> Indeed, contrary to the expected “blip” shape (Figure 1), here the current spikes present a symmetrical and sharp shape for a time ranging between 0.2 and 0.5 s. This result indicates that mechanism occurring during single vesicle collisions at Pt UME in the presence of an appropriate concentration of TX100 is probably different to those reported by Compton and Ewing at a carbon UME.<sup>6,7</sup> Moreover, this short time observed for current spikes suggests a quick releasing of the content against the Pt UME in a rapid electrolysis process. Thus, the electrolysis mechanism of the DMPC vesicles content during the collision at the Pt ultramicroelectrode surface in the presence of surfactant seems more

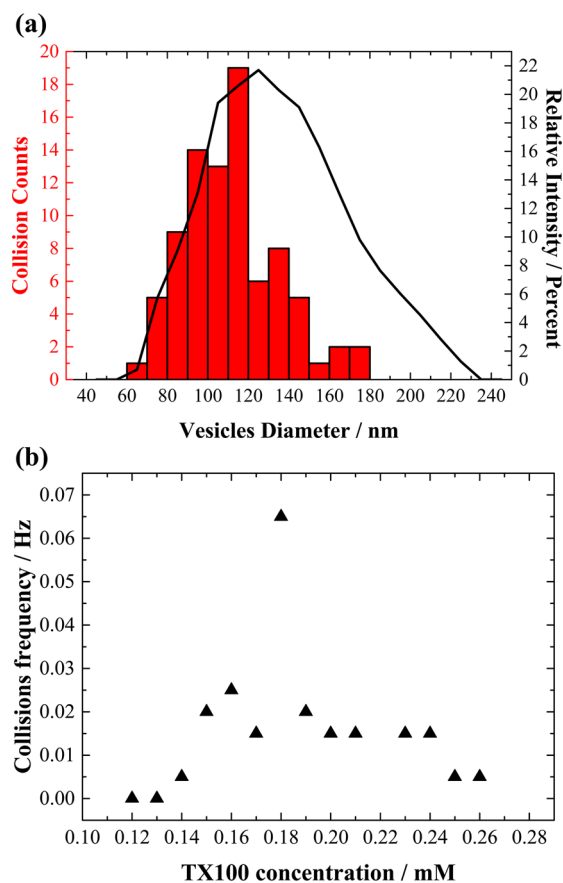


**Figure 4.** (a) Size distributions from DLS data (black line) and from charge data by integrating current spikes of  $i-t$  curve recorded at +0.6 V vs Ag/AgCl on 1.7  $\mu\text{m}$  Pt UME in 2 mL of 0.1 M KPB aqueous solution at pH 7 in the presence of 20  $\mu\text{L}$  of DMPC vesicles aqueous solution and 0.2 mM TX100 surfactant (red bar). (b) Collisions frequency determined from  $i-t$  curves of collision experiments by vesicles reactor method recorded at +0.6 V vs Ag/AgCl on 1.0  $\mu\text{m}$  Pt UME in 2 mL of 0.1 M KPB aqueous solution at pH 7 in the presence of 10  $\mu\text{L}$  of redox DMPC vesicles aqueous solution after addition of small TX100 concentrations every 5 min. The unusual single unique maximum point was seen in three trials (Figure S6) where it varied over a range of 0.05 mM.

complicated than a simple releasing process and probably requires additional studies to improve the understanding.

As previously shown in the VB technique, the vesicles concentration ( $C_{\text{ves}}$ ) can be calculated by using eqs 1 and 2 based on 120 nm diameter vesicles (determined by DLS measurement in Figure S1 and NTA data in Figure S2). Hence, the concentration of the pure redox DMPC vesicles aqueous solution before dilution is evaluated at  $4.4 \pm 0.1$  nM, a value close to that determined by NTA (Figure S2) at  $3.3 \pm 0.2$  nM and also in good agreement with the vesicles concentration determined by the VB method (Figure 2). This result indicates again that migration effects are less significant than diffusion, which is expected because very little faradaic current is flowing during VR experiments.<sup>29</sup>

Moreover, to confirm that current spikes are due to oxidation of  $\text{Fe}(\text{CN})_6^{4-}$  contained inside the vesicle during its collision, we can estimate the diameter of each vesicle from the charge obtained by calculating the charge passed during the collision, which corresponds to the amount of ferrocyanide oxidized and using Faraday's law. Here, we assume that the initial



concentration of ferrocyanide introduced into the vesicle solutions before extrusion is the same in each vesicle (i.e., an attoliter aliquot of the original solution), and we also assume that the electrode consumes all of the contents of the vesicle. In addition, we considered the cutoff for a “signal” (current spike) when the spike was at least three times the background noise in current. A background experiment without redox species inside DMPC vesicles (Figure S5) showed no current spike.

Thus, the vesicle diameter ( $d_{\text{ves}}$ ) can be calculated by eq 3:

$$d_{\text{ves}} = 2^3 \sqrt[3]{\frac{3Q}{4\pi n_e F C_{\text{redox}}}} \quad (3)$$

where  $Q$  is the measured charge,  $n_e$  is the number of electrons transferred during the electrolysis,  $n_e = 1$ ,  $F$  is Faraday's constant, and  $C_{\text{redox}}$  is the concentration of redox species encapsulated in vesicle,  $C_{\text{redox}} = 0.5$  M.

The overlay presented in Figure 4a showed that the size distributions from DLS data and calculated data were quite similar. Indeed, the DLS data indicated that the peak diameter is  $120 \pm 30$  nm (Figure S1) while the calculated data gave  $116 \pm 63$  nm as mean diameter from the corresponding average charge estimated at 0.079 pC. According to this result, the previous assumptions about the complete electrolysis and the expected concentration of ferrocyanide encapsulated inside vesicles (0.5 M) can be validated and, in addition, that showed the TX100 surfactant does not act on the size distribution of vesicles (nor on the consumed charge) during their collision.

As expected, the VR technique confirmed its efficiency to determine the size distribution of nanometer-sized vesicles and was also relevant to approximate the vesicles concentration in solution. Nevertheless, this last technique provided clear evidence observation of current spikes from these vesicles on a Pt UME necessitated a surfactant, such as TX100, in a controlled concentration. Indeed, TX100 is one of the most widely used nonionic surfactants to permeate the living cell membrane for transfection.<sup>21,24</sup> In fact, the transfection process consists to the opening of pores or holes in the BLM to allow the hydrophilic species adsorption/desorption of the vesicle content without damaging the membrane.<sup>24</sup> The study of TX100 surfactant concentration effect on the redox DMPC vesicle collisions frequency by detection of corresponding current spikes on Pt UME is presented in Figure 4b to determine the appropriate TX100 concentration to use.

Figure 4b shows the evolution of the collisions frequency versus the TX100 concentration added every 5 min in the redox DMPC vesicles aqueous solution by recording a chronoamperometric  $i-t$  curve (VR method) after each new addition. Especially, a chronoamperometric  $i-t$  curve like the one presented in Figure 3 is recorded on 300 s every 5 min (after each new addition of TX-100) on a fresh and clean Pt UME, and the collisions frequency (number of collisions during 300 s) is reported in Figure 4b for each TX-100 concentration added. The collisions frequency began at 0 Hz for TX100 concentrations below 0.14 mM and increased until the appropriate TX100 concentration at 0.18 mM provided a maximum frequency value of 0.065 Hz. These concentration values are in good agreement with the previous work of Koley and Bard reporting the TX100 concentration effects on membrane permeability of a single HeLa cell, where the TX100 critical micelle concentration (CMC) was evaluated at 0.17 mM.<sup>21</sup> According to their study, if the TX100 concentration is above this CMC (>0.18 mM), the cell

membrane is irreversibly damaged. Indeed, above 0.18 mM in Figure 4b, the collisions frequency quickly decreased, and after 0.25 mM TX100 almost no current spike was detected, suggesting the fatal breaking of the vesicles lipid bilayer. Unfortunately, the concentration of ferrocyanide released in solution following the prospective collapsing of all vesicles is too low ( $\sim 7 \mu\text{M}$ ) for inducing a significant difference on the background steady state current in 0.1 M KPB aqueous solution. Several experiments have been performed concerning the TX100 concentration effect on single vesicle collisions, and in all cases the collisions frequency curves versus the TX100 concentration (Figure S6) have presented the same trend observed in Figure 4b with a rapid increase at the appropriate TX100 concentration value around  $0.20 \pm 0.03$  mM. Moreover, all chronoamperometric  $i-t$  curves recorded in these conditions showed the same shape and size of current spikes confirming that surfactant does not disturb the electrolyzed content (integrated charge). Here, the TX100 effect on the vesicles BLM permeability could be explained by a process that involves the more facile release of the ferrocyanide content only during vesicle collision.

Finally, our study showed for the first time that a concentration around  $0.20 \pm 0.03$  mM of TX100 surfactant (dependent on the reaction time) in solution is essential and efficient to detect DMPC vesicles reactor collision events at the Pt UME hydrophilic surface.

## CONCLUSION

In summary, we have investigated vesicle behavior composed of a phospholipid bilayer membrane on a Pt ultramicroelectrode surface by two electrochemical detection methods involving discrete collision events. For the first time, we have shown that the vesicle blocking method is a useful technique for observing the vesicle adhesion on the Pt UME surface and also to evaluate the vesicle concentration in solution. Furthermore, our results have confirmed that the vesicle reactor method can be used to determine the vesicle size distribution, but the addition of a surfactant like Triton X-100 is necessary to oxidize the DMPC vesicle content. Indeed, in the absence of surfactant, the BLM does not allow passage of the contents to the UME for electrolysis during the vesicle collision on the Pt UME and is also too thick for allowing electron transfer across the BLM. Therefore, we have shown that the required Triton X-100 concentration is about  $0.20 \pm 0.03$  mM depending on the DMPC vesicle concentration in solution and under these conditions the BLM is permeable to hydrophilic species such as potassium ferrocyanide. Finally, we have suggested a transfection mechanism from the surfactant to explain the current spikes occurring during vesicles reactor collisions at Pt ultramicroelectrode, but this assumption should be checked by extending this study to other surfactants commonly used for cell transfection and probably also to other encapsulated hydrophilic electroactive species.

## ASSOCIATED CONTENT

### Supporting Information

The Supporting Information is available free of charge on the ACS Publications website at DOI: 10.1021/acs.langmuir.5b03123.

Figures S1–S6 (PDF)

## ■ AUTHOR INFORMATION

## Corresponding Author

\*E-mail [ajbard@cm.utexas.edu](mailto:ajbard@cm.utexas.edu) (A.J.B.).

## Notes

The authors declare no competing financial interest.

## ■ ACKNOWLEDGMENTS

E.L. acknowledges the Defense Threat Reduction Agency (Grant HDTRA1-11-1-0005). E.L. also thanks Christophe Renault and Jiyeon Kim for their valuable advice. J.D. acknowledges the National Science Foundation Graduate Research Fellowship (Grant DGE-1110007). A.B. acknowledges the National Science Foundation (Grant CHE-1405248) and the Welch Foundation (Grant F-0021). L.W. acknowledges the Welch Foundation (Grant F-1722).

## ■ REFERENCES

- (1) Kim, B.-K.; Boika, A.; Kim, J.; Dick, J. E.; Bard, A. J. Characterizing Emulsions by Observation of Single Droplet Collisions—Attoliter Electrochemical Reactors. *J. Am. Chem. Soc.* **2014**, *136*, 4849.
- (2) Dick, J. E.; Renault, C.; Kim, B.-K.; Bard, A. J. Electrogenerated Chemiluminescence of Common Organic Luminophores in Water Using an Emulsion System. *J. Am. Chem. Soc.* **2014**, *136*, 13546.
- (3) Dick, J. E.; Renault, C.; Kim, B.-K.; Bard, A. J. Simultaneous Detection of Single Attoliter Droplet Collisions by Electrochemical and Electrogenerated Chemiluminescent Responses. *Angew. Chem., Int. Ed.* **2014**, *53*, 11859.
- (4) Kim, B.-K.; Kim, J.; Bard, A. J. Electrochemistry of a Single Attoliter Emulsion Droplet in Collisions. *J. Am. Chem. Soc.* **2015**, *137*, 2343.
- (5) Cheng, W.; Compton, R. G. Oxygen Reduction Mediated by Single Nanodroplets Containing Attomoles of Vitamin B12: Electrocatalytic Nano-Impacts Method. *Angew. Chem., Int. Ed.* **2015**, *54*, 7082.
- (6) Cheng, W.; Compton, R. G. Investigation of Single-Drug-Encapsulating Liposomes using the Nano-Impact Method. *Angew. Chem., Int. Ed.* **2014**, *53*, 13928.
- (7) Dunevall, J.; Fathali, H.; Najafinobar, N.; Lovric, J.; Wigström, J.; Cans, A.-S.; Ewing, A. G. Characterizing the Catecholamine Content of Single Mammalian Vesicles by Collision–Adsorption Events at an Electrode. *J. Am. Chem. Soc.* **2015**, *137*, 4344.
- (8) Dick, J. E.; Hilterbrand, A. T.; Boika, A.; Upton, J. W.; Bard, A. J. Electrochemical detection of a single cytomegalovirus at an ultramicroelectrode and its antibody anchoring. *Proc. Natl. Acad. Sci. U. S. A.* **2015**, *112*, 5303.
- (9) Toh, H. S.; Compton, R. G. Electrochemical detection of single micelles through 'nano-impacts'. *Chemical Science* **2015**, *6*, 5053.
- (10) Dick, J. E.; Renault, C.; Bard, A. J. Observation of Single-Protein and DNA Macromolecule Collisions on Ultramicroelectrodes. *J. Am. Chem. Soc.* **2015**, *137*, 8376.
- (11) Allen, J. B.; Aliaksei, B.; SeongJung, K.; JunHui, P.; Scott, N. T. In *Nanoelectrochemistry*; CRC Press: Boca Raton, FL, 2015; p 241.
- (12) Keller, C. A.; Kasemo, B. Surface Specific Kinetics of Lipid Vesicle Adsorption Measured with a Quartz Crystal Microbalance. *Biophys. J.* **1998**, *75*, 1397.
- (13) Dimitrievski, K.; Kasemo, B. Simulations of Lipid Vesicle Adsorption for Different Lipid Mixtures. *Langmuir* **2008**, *24*, 4077.
- (14) Hellberg, D.; Scholz, F.; Schauer, F.; Weitschies, W. Bursting and spreading of liposomes on the surface of a static mercury drop electrode. *Electrochem. Commun.* **2002**, *4*, 305.
- (15) Hellberg, D.; Scholz, F.; Schubert, F.; Lovrić, M.; Omanović, D.; Hernández, V. A.; Thede, R. Kinetics of Liposome Adhesion on a Mercury Electrode. *J. Phys. Chem. B* **2005**, *109*, 14715.
- (16) Agmo Hernández, V.; Scholz, F. Kinetics of the Adhesion of DMPC Liposomes on a Mercury Electrode. Effect of Lamellarity, Phase Composition, Size and Curvature of Liposomes, and Presence of the Pore Forming Peptide Mastoparan X†. *Langmuir* **2006**, *22*, 10723.
- (17) Agmo Hernández, V.; Niessen, J.; Harnisch, F.; Block, S.; Greinacher, A.; Kroemer, H. K.; Helm, C. A.; Scholz, F. The adhesion and spreading of thrombocyte vesicles on electrode surfaces. *Bioelectrochemistry* **2008**, *74*, 210.
- (18) Kannuck, R. M.; Bellama, J. M.; Durst, R. A. Measurement of liposome-released ferrocyanide by a dual-function polymer modified electrode. *Anal. Chem.* **1988**, *60*, 142.
- (19) Young, R. C.; Feldberg, S. W. Photoinitiated mediated transport of H3O+ and/or OH- across glycerol monooleate bilayers doped with magnesium octaethylporphyrin. *Biophys. J.* **1979**, *27*, 237.
- (20) Feldberg, S. W.; Armen, G. H.; Bell, J. A.; Chang, C. K.; Wang, C. B. Electron transport across glycerol monooleate bilayer lipid membranes facilitated by magnesium etiochlorin. *Biophys. J.* **1981**, *34*, 149.
- (21) Koley, D.; Bard, A. J. Triton X-100 concentration effects on membrane permeability of a single HeLa cell by scanning electrochemical microscopy (SECM). *Proc. Natl. Acad. Sci. U. S. A.* **2010**, *107*, 16783.
- (22) Fontaine, P.; Fauré, M. C.; Muller, F.; Poujade, M.; Micha, J.-S.; Rieutord, F.; Goldmann, M. Unexpected Stability of Phospholipid Langmuir Monolayers Deposited on Triton X-100 Aqueous Solutions. *Langmuir* **2007**, *23*, 12959.
- (23) le Maire, M.; Champeil, P.; Møller, J. V. Interaction of membrane proteins and lipids with solubilizing detergents. *Biochim. Biophys. Acta, Biomembr.* **2000**, *1508*, 86.
- (24) Gennuso, F.; Ferneti, C.; Tirolò, C.; Testa, N.; L'Episcopo, F.; Caniglia, S.; Morale, M. C.; Ostrow, J. D.; Pascolo, L.; Tiribelli, C.; Marchetti, B. Bilirubin protects astrocytes from its own toxicity by inducing up-regulation and translocation of multidrug resistance-associated protein 1 (Mrp1). *Proc. Natl. Acad. Sci. U. S. A.* **2004**, *101*, 2470.
- (25) Lanyi, J. K. Influence of electron transport on the interaction between membrane lipids and Triton X-100 in Halobacterium cutirubrum. *Biochemistry* **1973**, *12*, 1433.
- (26) Kim, J.; Izadyar, A.; Nioradze, N.; Amemiya, S. Nanoscale Mechanism of Molecular Transport through the Nuclear Pore Complex As Studied by Scanning Electrochemical Microscopy. *J. Am. Chem. Soc.* **2013**, *135*, 2321.
- (27) Kim, J.; Kim, B.-K.; Cho, S. K.; Bard, A. J. Tunneling Ultramicroelectrode: Nanoelectrodes and Nanoparticle Collisions. *J. Am. Chem. Soc.* **2014**, *136*, 8173.
- (28) Kwon, S. J.; Zhou, H.; Fan, F.-R. F.; Vorobyev, V.; Zhang, B.; Bard, A. J. Stochastic electrochemistry with electrocatalytic nanoparticles at inert ultramicroelectrodes—theory and experiments. *Phys. Chem. Chem. Phys.* **2011**, *13*, 5394.
- (29) Boika, A.; Thorgaard, S. N.; Bard, A. J. Monitoring the Electrophoretic Migration and Adsorption of Single Insulating Nanoparticles at Ultramicroelectrodes. *J. Phys. Chem. B* **2013**, *117*, 4371.
- (30) Einstein, A. Über die von der molekularkinetischen Theorie der Wärme geforderte Bewegung von in ruhenden Flüssigkeiten suspendierten Teilchen. *Ann. Phys.* **1905**, *322*, 549.
- (31) Kučerka, N.; Kiselev, M.; Balgavý, P. Determination of bilayer thickness and lipid surface area in unilamellar dimyristoylphosphatidylcholine vesicles from small-angle neutron scattering curves: a comparison of evaluation methods. *Eur. Biophys. J.* **2004**, *33*, 328.